Particle detectors, cavities, and the weak equivalence principle

Erickson Tjoa,[1,2,*] Robert B. Mann,[1,2,†] and Eduardo Martín-Martínez[3,2,4,‡]

[1]*Department of Physics and Astronomy, University of Waterloo, Waterloo, Ontario N2L 3G1, Canada*
[2]*Institute for Quantum Computing, University of Waterloo, Waterloo, Ontario N2L 3G1, Canada*
[3]*Department of Applied Mathematics, University of Waterloo, Waterloo, Ontario N2L 3G1, Canada*
[4]*Perimeter Institute for Theoretical Physics, 31 Caroline St N, Waterloo, Ontario N2L 2Y5, Canada*

(Received 19 July 2018; published 4 October 2018)

We analyze a quantum version of the weak equivalence principle, in which we compare the response of a static particle detector crossed by an accelerated cavity with the response of an accelerated detector crossing a static cavity in $(1+1)$-dimensional flat spacetime. We show, for both massive and massless scalar fields, that the nonlocality of the field is enough for the detector to distinguish the two scenarios. We find this result holds for vacuum and excited field states of different kinds and we clarify the role of field mass in this setup.

DOI: 10.1103/PhysRevD.98.085004

I. INTRODUCTION

The weak equivalence principle (WEP) has been one of the central tenets of gravitational physics. It has a variety of formulations, but it asserts that the local effects of motion in a curved spacetime cannot be distinguished from those of an accelerated observer in flat spacetime. The proviso of locality eliminates measurable tidal forces (that would originate, e.g., from a radially convergent gravitational field) acting upon finite-sized physical bodies. It implies that the trajectories of bodies with negligible gravitational binding energy are independent of their composition and structure, and depend only their initial positions and velocities.

With the development of the Unruh-DeWitt (UDW) model in quantum field theory, the WEP can be analyzed in the presence of quantum fields in contrast to the original classical formulation. While not equivalent to a full quantum version of the WEP, this approach provides an operational means of understanding some important aspects of the WEP in a quantum context. In particular, since UDW detectors capture fundamental features of the light-matter interaction for atomic systems [1], one can operationally study the WEP by asking if a free-falling detector in a stationary cavity in a uniform gravitational field has a different response from that of a stationary detector surrounded by a free-falling cavity. This problem has recently been revisited in the context of moving mirrors [2].

Renewed effort has been expended in recent years towards reanalyzing the role of atomic detector models coupled to a real scalar field with regards to the connection to gravitational phenomena. It has been argued that noninertiality can be distinguished locally by exploiting nonlocal correlations of the field [3–5], effectively providing an accelerometer. An analysis of the behavior of a UDW detector in a static cavity indicated that quantum field theory may provide a way of distinguishing between flat-space acceleration and free fall in the near-horizon regime [4]. More recently [6] atoms falling through a cavity near an event horizon, together with short-wavelength approximations, led to radiation that is Hawking-like as seen by observers at spatial infinity. Even more recently, an analysis of a moving mirror in a cavity [2] has been used to argue once and for all that a "qualitative WEP" should hold in a quantum-field-theoretic setting, and emphasized the importance of the initial state of the field in determining radiation from a moving mirror. This investigation focused on mirrors lacking internal degrees of freedom, but nonetheless had the advantage of providing information about the stress-energy tensor in the cavity, which was apparently missed in the past.

Here we will complement these recent studies by showing that atomic UDW detectors also exhibit a qualitative WEP. In particular, we revisit the old problem of computing the response of a static detector surrounded by an accelerating cavity, and the response of an accelerating detector that is surrounded by a static cavity. The key issue here is not the composition of the detector (the body), but rather of its quantum field (vacuum) environment. We consider the response for various field states, including the (scalar) vacuum, excited Fock states, and also single-mode coherent field states. We find that the mass of the quantum scalar field does not enter into the response of the detector apart from providing a degradation in the transition amplitude and larger mode frequencies in the mode decomposition. This is

*e2tjoa@uwaterloo.ca
†rbmann@uwaterloo.ca
‡emartinmartinez@uwaterloo.ca

a consequence of the fact that the conformal invariance of the massless Klein-Gordon equation is not a physical effect, and is to be distinguished from the *conformal flatness* of the spacetime under consideration. For nonvacuum field states, we show how resonance can be used to amplify the transition probability via corotating terms and demonstrate the irrelevance of the mass of the field in the physics underlying the WEP.

Our paper is organized as follows. In Sec. II, we revisit the formulation of the WEP and clarify the contexts in which this work and others, in particular Refs. [2,6], are performed. In Sec. III we provide the standard setup and generic expressions for a UDW detector coupled to a Klein-Gordon field, without restriction to the vacuum state of the field. In Sec. IV we consider an accelerating detector traversing the entire static cavity, noting the necessary changes if the detector starts accelerating somewhere within the cavity. In Sec. V we consider a static UDW detector that encounters an accelerating cavity, entering one end and leaving the other due to the motion of the cavity; we also note the necessary modifications if the trajectory of the detector is changed. In Sec. VI we consider various nonvacuum field excitations and the role of resonance between atomic gap and excited cavity modes. In Sec. VII we compute the transition rate to better understand if the difference between two scenarios are not averaged out by the transition probability calculations.

Throughout we adopt $c = \hbar = 1$ so that the mass parameter m has units of inverse length.

II. WEAK EQUIVALENCE PRINCIPLE REVISITED

It is a remarkable property of gravity, in contrast to other nongravitational forces, that every test particle equally and universally experiences the influence of gravitational fields. This underlies the WEP, which states that the phenomenology of bodies observed from frames in uniform gravitational fields is equivalent to that of frames that accelerate uniformly relative to inertial (free-falling) frames [7]. In other words, the WEP states that a mass free falling in a stationary cavity with uniform gravitational field $\boldsymbol{g} = -g\boldsymbol{e}_z$ is completely equivalent to a stationary mass with uniformly accelerating cavity[1] with $\boldsymbol{a} = g\boldsymbol{e}_z$, as shown in Fig. 1. This principle has been verified to great accuracy through various experiments and effectively sets inertial mass and gravitational mass to be equal.

The purely classical version of the WEP, while asserting that free fall is independent of a body's composition, does not consider internal quantum degrees of freedom of a body (unlike a qubit). For example, the body is considered to be uncharged and the space inside the cavity to be free of electromagnetic fields. The quantum version of the WEP essentially requires us to consider an atomic detector coupled to some field prepared in some state, as shown in Fig. 2. The state most closely resembling the classical environment of the WEP is the quantum vacuum. Other field states can of course be considered, but they will in general produce environments analogous to those of air or some other fluid that produces drag on the body. For example [2], having an electromagnetic field makes the argument less trivial: a classical electric charge in uniform accelerated motion radiates and it is nontrivial to ask whether a *free-falling* charge radiates. The reason is because in general relativity, free falling is an inertial motion (geodesic motion) and acceleration corresponds to nongeodesics in spacetime. According to the equivalence principle, however, we should be able to speak of uniform acceleration and constant gravitational fields incontrovertibly. Where is the problem?

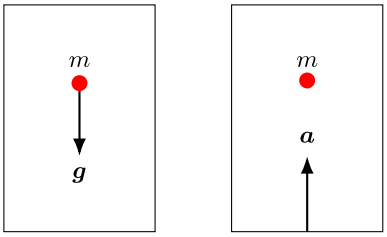

FIG. 1. Classical WEP setup: test mass m in a closed cavity. WEP claims that these two are kinematically indistinguishable in the absence of second-order effects such as tidal forces or nonuniform acceleration. The space inside the cavity is a true vacuum in the classical sense, apart from the existence of a gravitational field to mimic acceleration.

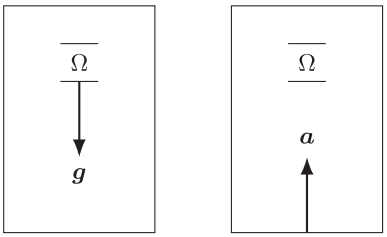

FIG. 2. Quantum WEP setup: a two-level atomic "detector" with gap Ω (with respect to its proper frame) in a cavity. The cavity contains a quantum field whose modes may lead to atomic excitations (even in the vacuum state), and hence detector responses. The atom serves as a detector in the sense that a particle is detected when the atom is excited and then emits radiation [8].

Here we revisit this problem using a UDW detector to replace the mirror in Ref. [2]. Specifically, we consider two different "Experiments":

(1) *Stationary cavity, accelerating detector:* In this scenario, we let an atomic detector undergo uniform acceleration as it crosses the cavity containing the

[1]Alternatively, the normal force experienced by a test mass on the floor of a closed cavity cannot be attributed to cavity acceleration or a uniform gravitational field without additional nonlocal information (e.g., by looking out of the cavity).

quantum field. This mimics the scenario of a free-falling atom in a gravitational field e.g., outside a black hole especially near the horizon, when the metric is approximately Rindler-like [6].

(2) *Stationary detector, accelerating cavity:* In this scenario, a rigid cavity is accelerating such that a stationary detector traverses across the cavity. This mimics a free-falling cavity in a gravitational field under appropriate quasilocal approximations.

If WEP holds, then we should expect that Experiment 1 and Experiment 2 should be qualitatively symmetric in some regimes for the scalar field vacuum. More generally, we might expect that for other field states that the motion of the body is independent of the field mass. In order to make useful and valid comparisons in the context of WEP, we generally need to ensure two additional "requirements" on the setup in question.

First of all, we will need to be able to set up a kind of cavity undergoing constant acceleration across its full spatial extent. This is forbidden in special relativity without abandoning the rigidity condition [9–11] (static boundary condition in Rindler coordinates). Therefore, a rigid accelerating cavity suitable for WEP is necessarily in a *quasilocal* regime in the sense of $aL \ll 1$ where L is the proper length of the cavity at rest as measured in the lab frame. Outside this regime, we see that the accelerating cavity will have detectable nonuniform proper accelerations across the cavity and hence in the comoving frame of the cavity, the stationary detector (with respect to lab frame) does *not* undergo uniform acceleration since the worldline of the detector crosses hypersurfaces of constant but different accelerations. Therefore, Experiment 1 and Experiment 2 are only equivalent in quasilocal approximations.

Second, we will need to show that the distinction between detector responses in Experiments 1 and 2 should be qualitatively independent of the mass of the quantum field and the initial state of the field within the quasilocal regime. In other words, *quantitative* differences between Experiments 1 and 2 would then be attributed to nonlocal correlations: the atom is sensitive to the inequivalent setups in the two experiments and also the fact that a moving boundary/stationary atom is not the same as a moving atom/stationary boundary from a physical point of view.

Furthermore, the role of the field mass should only serve to degrade nonlocal correlations of the field and hence diminish transition amplitudes, all else being equal. This requirement, however, is in slight tension with previous results [3] claiming (in the nonrelativistic regime) that the field mass term can enhance the transition probability of a detector, making it a better accelerometer in the case of highly excited field states. This would mean that the mass of a scalar field leads to additional physical effects *beyond* suppressing correlations. For the WEP in particular, one could imagine increasing the mass more and more to detect increasingly small local accelerations. We will recover consistency with WEP by showing that this discrepancy is in part due to mixing conformal flatness with conformal invariance of the Klein-Gordon equation. We also note that the idea that massive excitations should be "harder" to detect than the massless ones, all things being equal, is not new; it has been investigated e.g., in Ref. [12]. A more complete discussion of these issues is given in Appendices A and B.

In light of these two requirements, in the next few sections we will consider the setup and demonstrate that the qualitative WEP is indeed observed. In particular, we recover the expectation that a massless field should be able to detect relative acceleration (noninertiality) as well as the massive field, if not better, in the quasilocal regime. This entails the clarification that conformal invariance in the massless case has nothing to do with the physics of uniform acceleration and hence WEP; it is a computational convenience that one can invoke (cf. Appendix A), to be distinguished from the fact that all two-dimensional spacetimes are conformally flat. We will strengthen this claim by considering an arbitrary Fock state and a single-mode coherent state, and check that no essential differences arise even in the transition rate (which is a differential version of the detector response).

III. SETUP

Our starting point is the Klein-Gordon equation for a real scalar field: the covariant formulation of the Klein-Gordon equation which governs the dynamics of a real scalar field reads

$$\frac{1}{\sqrt{-g}}\partial_\mu(g^{\mu\nu}\sqrt{-g}\partial_\nu\phi) + m^2\phi = 0. \tag{1}$$

For global Minkowski spacetime, the solutions are given by plane waves. Recall that all $(1+1)$-dimensional spacetimes are conformally equivalent to Minkowski spacetime: by this we mean that *there exists* a coordinate system in which the metric is conformally flat, i.e., with a metric that takes the form

$$g_{\mu\nu}(\mathsf{x}) = \Omega^2(\mathsf{x})\eta_{\mu\nu}. \tag{2}$$

This conformal flatness can be exploited in the case of $m = 0$ to map the solutions of the Klein-Gordon equation to the plane-wave solutions in Minkowski spacetime because the massless Klein-Gordon equation is conformally invariant in $(1+1)$ dimensions. This allows us to obtain an *exact closed form* for the spectrum of the field modes.[2] For $m \neq 0$, the conformal invariance of the wave equation is lost and hence conformal flatness provides no particular advantage. Therefore, even for a uniformly

[2]An important point here is that conformal invariance is convenient but not necessary. We show this in Appendix A.

accelerating frame the field modes can be written in closed form; however neither the normalization nor the spectrum can.

To probe the field, we consider a pointlike UDW detector whose interacting Hamiltonian is given by

$$\hat{H}_I(\tau) = \lambda\chi(\tau)\hat{\mu}(\tau)\hat{\phi}(\tau, x(\tau)),$$
$$\hat{\mu} = e^{i\Omega\tau}\hat{\sigma}^+ + e^{-i\Omega\tau}\hat{\sigma}^-, \tag{3}$$

where τ is the proper time of the detector, λ is the coupling strength of the detector and the field, $\hat{\mu}(\tau)$ is the monopole moment of the detector, $\hat{\sigma}^\pm$ are $\mathfrak{su}(2)$ ladder operators characterizing the two-level atomic detector, and $\chi(\tau)$ is the switching function of the detector. Here $\hat{\sigma}^+|g\rangle = |e\rangle$ and $\hat{\sigma}^-|e\rangle = |g\rangle$ where $|g\rangle$, $|e\rangle$ refer to the ground and excited states of the atom respectively, separated by the energy gap Ω. Note that the interacting Hamiltonian is given in the Dirac picture.

We consider the initial state to be a separable state $|g\rangle \otimes |\psi\rangle = |g, \psi\rangle$ where $|\psi\rangle$ is some initial pure state of the field. If the field is in some $|\text{out}\rangle$ state after the interaction and the detector is in an excited state $|e\rangle$, then the transition probability of the detector is given by Born's rule after tracing out the field state:

$$P(\Omega) = \sum_{\text{out}} |\langle e, \text{out}|\hat{U}|g, \psi\rangle|^2 \tag{4}$$

where the time evolution operator in the Dirac picture is

$$\hat{U} = \mathcal{T}\exp\left(-\frac{i}{\hbar}\int_{-\infty}^{\infty} d\tau \hat{H}_I(\tau)\right). \tag{5}$$

Employing the Dyson expansion

$$\hat{U} = \hat{\mathbb{1}} + \hat{U}^{(1)} + O(\lambda^2),$$
$$\hat{U}^{(1)} = -\frac{i}{\hbar}\int_{-\infty}^{\infty} d\tau \hat{H}_I(\tau) \tag{6}$$

we obtain the leading-order contribution to the transition probability

$$P(\Omega) = \lambda^2 \int d\tau \int d\tau' \chi(\tau)\chi(\tau')e^{-i\Omega(\tau-\tau')}W(\tau,\tau') + O(\lambda^4),$$
$$W(\tau,\tau') = \langle\psi|\hat{\phi}[\mathsf{x}(\tau)]\hat{\phi}[\mathsf{x}(\tau')]|\psi\rangle, \tag{7}$$

where $W(\tau, \tau')$ is the pullback of the Wightman function on the detector's trajectory $\mathsf{x}(\tau)$. The remaining task is to compute the Wightman function for different scenarios and choose an appropriate switching function of the detector.

We would like to study further the situation when one speaks of the weak equivalence principle in the presence of a quantum field subject to a boundary condition (a Dirichlet cavity) in $(1+1)$ dimensions. We are interested in two types of scenarios ("Experiments") that can be summarized as follows:

(1) A cavity is static relative to some laboratory frame (t, x) and the detector is accelerating with constant proper acceleration. In the language of the equivalence principle, this should also describe a static cavity in a constant gravitational field (like on the surface of the Earth), with a free-falling detector.
(2) The detector is static relative to the lab frame and a *rigid* cavity uniformly accelerates, mimicking a free-falling cavity in a uniform gravitational field.

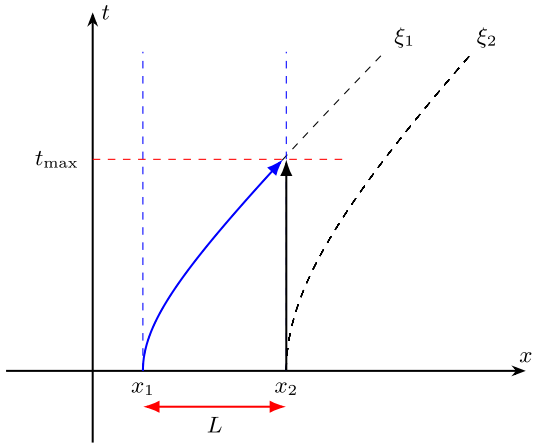

FIG. 3. Spacetime diagram for the setup under consideration. The accelerating detector–static cavity scenario corresponds to the trajectories in blue, with the accelerating detector denoted by the solid curved arrow. The accelerating (rigid) cavity–static detector scenario corresponds to the trajectories in black, with the static detector denoted by the solid vertical curve. In both scenarios the trajectories of the end points of the cavity are given by dashed lines.

The spacetime diagram for these two setups is shown in Fig. 3. Case 1) corresponds to the trajectories in blue, with the accelerating detector denoted by the solid curved arrow. Case 2) corresponds to the trajectories in black, with the static detector denoted by the solid vertical curve. In both scenarios the cavity trajectories are dashed lines.

We will see that this result continues to hold even for excited field states, including coherent states [13]. Therefore, this effectively shows that massive scalar fields do not generally provide additional insight over massless scalar fields, apart from introducing an additional degradation factor (e.g., in the studies of entanglement generation or degradation [14]).

IV. ACCELERATING DETECTOR

Let us first consider the case of a static cavity relative to the lab frame (t, x). In this case, the cavity is equivalent to a Dirichlet boundary condition $\phi(x_1) = \phi(x_2) = 0$ where x_j are the locations of the boundary and the length of the cavity as measured by the lab frame is $L = x_2 - x_1$.

The equation of motion for the quantized scalar field reduces to

$$(\partial_\mu \partial^\mu + m^2)\hat{\phi} = 0 \tag{8}$$

and under a Dirichlet boundary condition the modes are standing waves:

$$\hat{\phi}(t,x) = \sum_{n=1}^{\infty} u_n(x)(e^{-i\omega_n t}\hat{a}_n + e^{i\omega_n t}\hat{a}_n^\dagger),$$
$$u_n(t,x) = \frac{1}{\sqrt{L\omega_n}} \sin\frac{n\pi(x-x_1)}{L}, \tag{9}$$

where $\omega_n^2 = (\frac{n\pi}{L})^2 + m^2$. The normalization of u_n can be found using the Klein-Gordon inner product [8]

$$(\phi_1, \phi_2) = -i\int_\Sigma d\Sigma^\mu (\phi_1 \partial_\mu \phi_2^* - (\partial_\mu \phi_1)\phi_2^*), \tag{10}$$

where Σ is the spacelike hypersurface foliated by the global time function defining the timelike Killing vector of the spacetime.

For the detector/cavity configuration (see Fig. 3), if the detector is accelerating from the left wall to the right wall of the cavity then $x_1 = 0$; if the detector starts from the midpoint, then $x_1 = -L/2$. Starting at the midpoint (as in Ref. [3]) is useful if we wish to consider the $a = 0$ limit, since the Dirichlet boundary renders the limit ill-defined for a detector starting from the left where the field vanishes (i.e., the detector "merges" with the wall). We will consider trajectories in which the detector travels from one wall to the other as well as from the midpoint as appropriate; we shall refer to the latter kind of trajectory as a "midpoint trajectory."

If the initial state of the field is the Minkowski vacuum state $|0_M\rangle$, then it is straightforward to show that the pullback of the Wightman function along the trajectory $\gamma(\tau)$ is

$$W_0(\tau,\tau') = \sum_{n=1}^{\infty} u_n(\mathsf{x}(\tau))u_n^*(\mathsf{x}(\tau')). \tag{11}$$

For a uniformly accelerating detector, this trajectory is given by

$$\mathsf{x}(\tau) = \frac{1}{a}(\sinh a\tau, \cosh a\tau - 1) \tag{12}$$

where the integration constant is chosen so that $x(\gamma(0)) = 0$. Solving for the time taken to traverse the cavity, we obtain

$$\tau_{\max} = \frac{\cosh^{-1}(1+aL)}{a}. \tag{13}$$

If the detector starts from the midpoint of the cavity, then the expression for the time to exit the cavity is given by Eq. (13) with $L \to L/2$. Finally, putting everything together, we obtain

$$P_0^D(\Omega) = \lambda^2 \sum_{n=1}^{\infty} \frac{1}{L\omega_n}\left|\int_{-\infty}^{\infty} d\tau \chi(\tau) \sin\frac{n\pi}{L}\left(\frac{\cosh a\tau - 1}{a} - x_1\right)\right.$$
$$\left. \times e^{-i\Omega\tau} \exp\left(-i\omega_n \frac{\sinh a\tau}{a}\right)\right|^2 \tag{14}$$

for the detector transition probability for the field in the vacuum state. Note that the limits of integration are effectively governed by the switching function. We shall generally choose $\chi(\tau) = 1$ for the interval $[0, \tau_{\max}]$ and zero otherwise (the so-called top-hat switching). We use the superscript D to denote an accelerating detector in a cavity that is static with respect to the lab frame (t, x); otherwise we use the superscript C. Note that the cavity forces the field to be compactly supported in the interval $[x_1, x_2]$, beyond which the detector experiences no interaction with the field.

We remark that for a trajectory where the detector traverses the entire cavity (from one wall to another), the divergences associated with sudden switching do not occur because the Dirichlet boundary condition causes the field to vanish there (see for instance Ref. [15]). Effectively, the detector does not see the discontinuity in the switching. Furthermore, while divergences due to sudden switching arise in quite general contexts [16], it is also now known that the spurious divergence due to sudden switching in Minkowski space is in fact dimension dependent [17] and the $(1+1)$-dimensional setup does not suffer from this problem due to the logarithmic nature of the singularity in the Wightman function. Since the mode sum is convergent even without a UV regulator, imposing a UV cutoff is a computational convenience (cf. Appendix C). An IR cutoff naturally arises from the Dirichlet boundary condition; thus the usual divergence of a massless scalar field in $(1+1)$ dimensions does not appear either.

V. ACCELERATING CAVITY

Now suppose we consider a rigid cavity of length L as measured in the lab frame at $t = 0$. The cavity is uniformly accelerating in the positive x direction, and there is an inertial UDW detector at rest at (t, x_d) where x_d is constant. This corresponds to the detector passing through a cavity with moving boundary conditions. In $(1+1)$ dimensions, there is an analytic solution to this seemingly difficult problem $m = 0$: we perform a coordinate transformation

$$t = \frac{e^{a\zeta}}{a}\sinh a\varsigma, \qquad x = \frac{e^{a\zeta}}{a}\cosh a\varsigma \tag{15}$$

where (ς, ζ) are sometimes known as the Lass or radar Rindler coordinates [18]; we will refer to these as

conformal Rindler coordinates. This coordinate system covers the usual Rindler wedge and has the special property that the metric is conformal to the Minkowski metric:

$$\mathrm{d}s^2 = \mathrm{d}t^2 - \mathrm{d}x^2 = e^{2a\zeta}(\mathrm{d}\varsigma^2 - \mathrm{d}\zeta^2). \tag{16}$$

Each line of constant ζ describes a uniformly accelerating trajectory with proper acceleration $|a^\mu a_\mu|^{1/2} = ae^{-a\zeta}$. Consequently the kinematical parameter a for the line $\zeta = 0$ corresponds to the proper acceleration of the test particle along this trajectory. In these coordinates, the cavity walls correspond to Dirichlet boundary conditions at $\zeta = \zeta_1, \zeta_2$. Since we are comparing the scenarios in which the detector traverses the entire cavity, we will also choose $\zeta_1 = 0$ so that the proper acceleration of the left wall matches the acceleration of the detector.[3] Inverting the coordinates, the trajectory of the static detector is

$$\varsigma = \frac{1}{a}\tanh^{-1}\frac{t}{x_d}, \qquad \zeta = \frac{1}{a}\log a\sqrt{x_d^2 - t^2}. \tag{17}$$

If we define the left wall to be at $\zeta = \zeta_1 = 0$, then the proper length of the cavity in conformal coordinates is

$$L = x_2 - x_1|_{t=0} = \int_{\zeta_1=0}^{\zeta_2 := L'} \mathrm{d}\zeta e^{a\zeta} = \frac{e^{aL'} - 1}{a}, \tag{18}$$

which can be inverted to give $L' = a^{-1}\log(1 + aL)$. Crucially, $x_2 - x_1 \neq \zeta_2 - \zeta_1$. If the detector starts at the right wall and the cavity accelerates in the positive x direction, then we have $x_d = a^{-1} + L$. The maximum interaction time is obtained by solving for

$$a\sqrt{x_d^2 - t^2} = 1 \Rightarrow t_{\max} = \sqrt{\frac{2L}{a} + L^2}. \tag{19}$$

For the massless field, the Klein-Gordon equation is conformally invariant under the above transformation and hence the modes in this coordinate system read

$$\hat{\phi}(\varsigma, \zeta) = \sum_{n=1}^{\infty} v_n(\zeta)(e^{-i\tilde{\omega}_n\varsigma}\hat{b}_n + e^{i\tilde{\omega}_n\varsigma}\hat{b}_n^\dagger), \tag{20}$$

$$v_n = \frac{1}{\sqrt{n\pi}}\sin\frac{n\pi(\zeta - \zeta_1)}{L'}, \tag{21}$$

where we have used the fact that the normalization simplifies due to $\sqrt{L'\tilde{\omega}_n} = \sqrt{n\pi}$. Note that $L' \neq L$ since conformal transformation does not preserve length, i.e., the comoving length of the cavity in radar coordinates is $\zeta_2 - \zeta_1 \neq L$.

Since $t = \tau$ is the proper time, the full transition probability for traversing the entire cavity is

$$P_0^C(\Omega) = \lambda^2\sum_{n=1}^{\infty}\left|\int_{-\infty}^{\infty}\mathrm{d}\tau\chi(\tau)\sin\frac{n\pi\log\sqrt{(1+aL)^2 - a^2\tau^2}}{\log 1 + aL} \times e^{-i\Omega\tau}\exp\left(-\frac{in\pi\tanh^{-1}\frac{a\tau}{1+aL}}{\log(1+aL)}\right)\right|^2, \tag{22}$$

with the top-hat switching in the interval $[0, \tau_{\max}]$, noting that here $t_{\max} = \tau_{\max}$.

If the detector trajectory is such that at $t = 0$ it is at the midpoint of the cavity ("midpoint detector"), then some parts of these expressions will need to be changed if we want the kinematical parameter a to be the proper acceleration at the center of the cavity (such as was done in Ref. [3]). Both $t_{\max}$ and L' will change for the midpoint detector

$$L' = \log\frac{2 + aL}{2 - aL}, \qquad t_{\max} = \sqrt{\frac{L}{a} - \frac{L^2}{4}} \tag{23}$$

and there will be a slight modification of Eq. (22). Also, clearly ζ_1 would not be zero in this case.

If the field is massive, the Klein-Gordon equation is no longer invariant under a conformal transformation, and it is more advantageous to use the manifestly simpler standard Rindler coordinates

$$t = \xi\sinh\eta, \qquad x = \xi\cosh\eta. \tag{24}$$

Let us work this out explicitly from the Klein-Gordon equation: since $\sqrt{-g} = \xi$, the covariant Klein-Gordon equation gives

$$\frac{1}{\xi^2}\frac{\partial^2\phi}{\partial\eta^2} - \left(\frac{1}{\xi}\frac{\partial\phi}{\partial\xi} + \frac{\partial^2\phi}{\partial\xi^2}\right) + m^2\phi = 0. \tag{25}$$

Separating variables $\phi = v(\xi)T(\eta)$, we can show that $T(\eta) \propto \exp\pm i\omega\eta$ and hence we obtain the modified Bessel differential equation of imaginary order for the spatial mode $v(\xi)$:

$$\xi^2\frac{\partial^2 v}{\partial\xi^2} + \xi\frac{\partial v}{\partial\xi} + (\omega^2 - m^2\xi^2)v = 0. \tag{26}$$

Implementing the Dirichlet boundary condition $v(\xi_1) = v(\xi_2) = 0$ as before, the modes will have a discrete

[3]Note that if we consider the midpoint of the cavity to have acceleration a, then it is *not* true that the walls are located at $\zeta_j = \pm L'/2$: conformal transformations do not preserve distances between two points. In particular, it can be shown that

$$x_j = \frac{1}{a} \pm \frac{L}{2} \Rightarrow \zeta_j = \log\left(1 \pm \frac{aL}{2}\right)$$

which is manifestly not symmetric with respect to the detector position $\zeta_d = 0$.

spectrum labeled by $n \in \mathbb{Z}$ and the spatial mode can be expressed in terms of modified Bessel functions of imaginary order [19]:

$$v_n(\xi) = |A_n|(\mathrm{Re}(I_{i\omega_n}(m\xi_1))K_{i\omega_n}(m\xi) - \mathrm{Re}(I_{i\omega_n}(m\xi))K_{i\omega_n}(m\xi_1)),$$
$$1 = 2|A_n|^2\omega_n \int_{\xi_1}^{\xi_2} \frac{\mathrm{d}\xi}{\xi}|v_n(\xi)|^2, \tag{27}$$

where the normalization follows from the Klein-Gordon inner product in Eq. (10). The discrete spectrum and the normalization must be solved numerically. Similar to the massless case, we can then do the pullback of the Wightman function onto the trajectory of the detector which is given by

$$\xi(\tau) = \sqrt{x_d^2 - t^2}, \qquad \eta(\tau) = \tanh^{-1}\frac{t}{x_d} \tag{28}$$

where the constant x_d describes the static detector trajectory with respect to the lab coordinates.

We pause to comment about rigid-body motion in the Rindler frame. Note that even if the acceleration of the leftmost wall becomes arbitrarily large, the center-of-mass acceleration is bounded above by the rigidity condition: a rigid cavity of length L in the lab frame must have a different proper acceleration at each point in order to remain rigid. The proper acceleration at any point x within the cavity is given by

$$a(x) = \frac{a_1}{1 + a_1(x - x_1)}, \tag{29}$$

where $x_1 = a_1^{-1}$ is the location of the left wall and a_1 is the proper acceleration of the left wall. We see that at the center $x_c = a_1^{-1} + L/2$ of the cavity we have the limit

$$\lim_{a_1\to\infty} a_c = \lim_{a_1\to\infty} \frac{2a_1}{2 + a_1 L} = \frac{2}{L}. \tag{30}$$

If the center of the cavity attains an acceleration larger than this, the rear wall will cross the future Rindler horizon, which is an unphysical cavity setup.

Another way to see this geometrically is by looking at the spacetime diagram (cf. Fig. 3). For a uniformly accelerating rigid cavity, the two walls must both be on two different hypersurfaces of constant ξ in order for them to be a Dirichlet boundary i.e., $\xi = \xi_1$ and $\xi = \xi_2$. Different values of ξ correspond to trajectories with different proper accelerations, and the lab observer does not see this cavity as rigid because the cavity shrinks across the plane of simultaneity of constant t. The rigidity condition essentially means that the cavity has a constant length when measured in the plane of simultaneity of constant η.

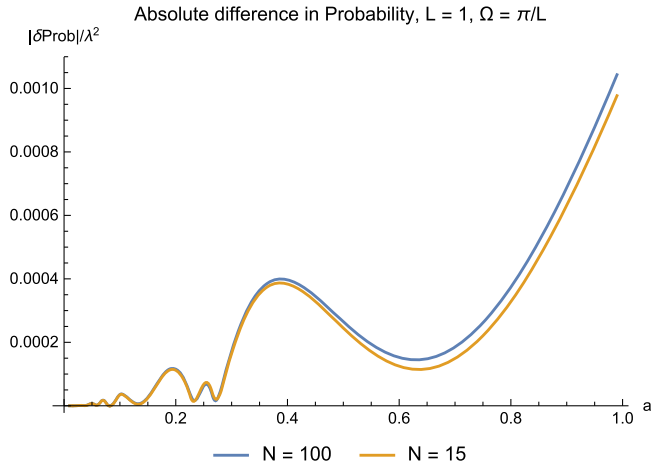

FIG. 4. Absolute difference in probability $|P_0^C - P_0^D|/\lambda^2$ as a function of acceleration for $\Omega = \pi/L$ for $M = 0$. Here and for subsequent plots we set $L = 1$ for convenience. For small accelerations, the mode sums quickly converge for small N and the difference in transition probability of the two scenarios is vanishingly small in the low-acceleration limit.

In Fig. 4 we plot the absolute probability difference between the accelerating cavity and the accelerating detector scenarios as a function of the proper acceleration a. A larger energy gap generally suppresses the transition probability in the massless scenario as shown in Fig. 5, and similar qualitative suppression is observed in the massive case. To compare the convergence of the mode sums, we considered ranging both $N = 15$ and $N = 100$. The larger value of N is required for larger acceleration parameters a (see also Appendix C for separate convergence checks).

In Fig. 6 we compare the absolute probability difference for massless and massive fields. Here our results agree with previous work [3] in that if the initial field state is the

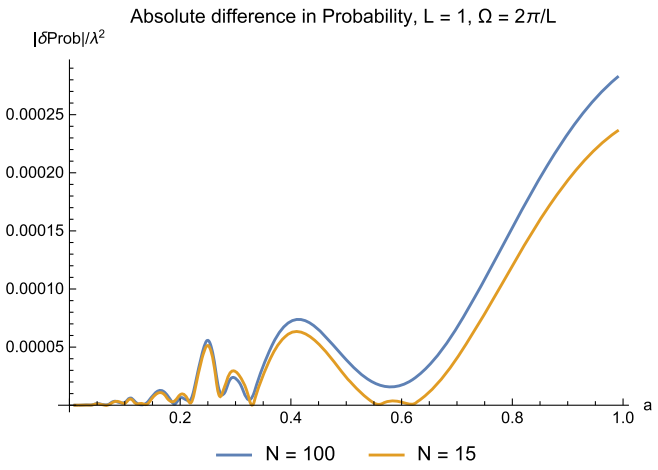

FIG. 5. Absolute difference in probability $|P_0^C - P_0^D|/\lambda^2$ as a function of acceleration for the larger gap $\Omega = 2\pi/L$, $L = 1$ for $m = 0$.

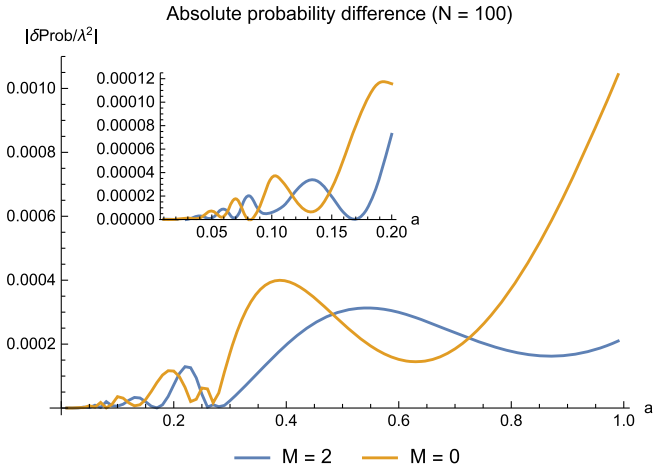

FIG. 6. Comparison of the absolute difference in probability $|P_0^C - P_0^D|/\lambda^2$ as a function of acceleration for $L = 1$, $\Omega = \pi/L$ when the field is initially in the vacuum state. Here $L = 1$ for convenience. The difference between an accelerating cavity and an accelerating detector vanishes quickly at low accelerations.

vacuum, then for $aL \ll 1$ the difference in responses between inertial and noninertial detectors quickly vanishes. For completeness, we plot in Fig. 7 the transition probability of the accelerating cavity scenario for very small mass. We see that indeed it provides the correct massless limit despite the rather complicated mode functions involving modified Bessel functions. The accelerating detector case will trivially have the correct limit since the functional form of the Wightman functions is the same.

Furthermore, we do see a considerable distinction between the massive and massless cases once a becomes

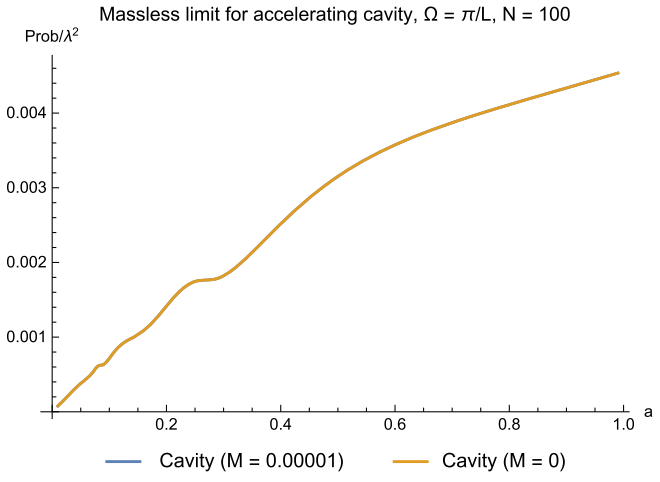

FIG. 7. Transition probability (divided by λ^2) as a function of acceleration for $\Omega = \pi/L$, $L = 1$, showing that in the small mass limit the results agree with the massless case. We choose $N = 100$ instead of the value $N = 15$ as in previous plots. Note that a value of $M = 0.0001$ is small enough to be indistinguishable from the $M = 0$ case, with a relative difference in probability of 2 parts in a billion (10^{-9}) at $a \approx 0.01$.

sufficiently large (cf. Fig. 6). The larger difference in response for the two setups at large a should not be taken to be a fundamental violation of the WEP: for large a, the nonuniformity of the cavity acceleration at different points is more pronounced, similar to how the nonuniformity of Earth's gravitational field is detectable if we consider a large enough region in space.

VI. EXCITED FIELD STATES

After considering the vacuum state of the field, a natural question arises: can sensitivity to noninertiality be enhanced if the field state is not a vacuum state? The additional terms in the Wightman function due to the excited field states may have a corotating term of the form $\Omega - \omega_n$ which may produce resonant-like behavior, while for the vacuum state this cannot occur for a ground state atom. We will consider both single-mode excited Fock states and single-mode coherent states.

A. Single-mode excited Fock state

The simplest excited field state we can consider is a single-mode nonvacuum Fock state, i.e., when the kth momentum has n_k excitations. This is a straightforward generalization from the expression found in Ref. [3]. We denote this by $|n_k\rangle$ which formally reads $|n_k\rangle \sim |000\ldots 0n_k 000\ldots\rangle$, where the enumeration is formally valid because of the countably infinite spectrum. The corresponding Wightman function is formally given by

$$W(\mathsf{x},\mathsf{x}') = \langle n_k|\phi(\mathsf{x})\phi(\mathsf{x}')|n_k\rangle. \tag{31}$$

Employing the result

$$\begin{aligned}\phi(\mathsf{x}')|n_k\rangle = &\sum_{l\neq k} u_l^*(\mathsf{x}')|1_l, n_k\rangle + \sqrt{n_k+1}\,u_l^*(\mathsf{x}')|n_k+1\rangle \\ &+ \sqrt{n_k}\,u_l(\mathsf{x}')|n_k-1\rangle\end{aligned} \tag{32}$$

where the $\{u_j\}$ are the eigenmodes of the Klein-Gordon equation (not just the spatial part), we obtain

$$\begin{aligned}W(\mathsf{x},\mathsf{x}') &= \sum_{j,l\neq k} u_j(\mathsf{x})u_l^*(\mathsf{x}') + (n_k+1)u_k(\mathsf{x})u_k^*(\mathsf{x}') \\ &\quad + n_k u_k^*(\mathsf{x})u_k(\mathsf{x}') \\ &= \sum_j u_j(\mathsf{x})u_j^*(\mathsf{x}') + n_k u_k(\mathsf{x})u_k^*(\mathsf{x}') \\ &\quad + n_k u_k^*(\mathsf{x})u_k(\mathsf{x}') \\ &= W_0(\mathsf{x},\mathsf{x}') + W_{\rm exc}(\mathsf{x},\mathsf{x}')\end{aligned} \tag{33}$$

for the full expression for the Wightman function. Therefore, for an excited field state given by a single-mode Fock state, the Wightman function is the sum of the vacuum Wightman function W_0 and an additional piece $W_{\rm exc}$ that is

explicitly dependent on which mode is excited. Since the transition probability is linear in $W(\mathsf{x},\mathsf{x}')$, we see that the transition probability for this state reads

$$P_{\rm tot}(\Omega) = P_0(\Omega) + n_k\left|\int {\rm d}\tau\chi(\tau)e^{-i\Omega\tau}u_k(\tau)\right|^2 + n_k\left|\int {\rm d}\tau\chi(\tau)e^{-i\Omega\tau}u_k^*(\tau)\right|^2. \quad (34)$$

We are interested in $W_{\rm exc}$ since we found W_0 in the previous section and we can always subtract off the vacuum contribution. Note that

$$e^{-i\Omega\tau}u_k(\tau) \sim e^{-i(\omega_k T(\tau)+\Omega\tau)},$$
$$e^{-i\Omega\tau}u_k^*(\tau) \sim e^{-i(\omega_k T(\tau)-\Omega\tau)}, \quad (35)$$

where $T(\tau)$ is the time function [which in our case is either $\eta(\tau)$ or $t(\tau)$] along the trajectory of the detector. The third term in $P_{\rm tot}$ is the "corotating term" which will tend to dominate over the second ("counter-rotating") term.

The above results teach us that there are two ways in which one can "neglect" the vacuum contribution. One is when we have an approximate *resonance* (up to some Doppler shifts) i.e., when $\Omega \sim \omega_k$. In this case, the resonance will amplify the transition rate and the vacuum contribution can be rendered negligible compared to the rest. The other is if there is a sufficiently higher number of excitations n_k: in this case the transition probability scales as

$$P_{\rm excited} \sim \frac{n_k}{k} \quad (36)$$

where the denominator $1/k$ comes from the normalization of u_k. This means for a given energy gap Ω, the higher-momentum mode will need an excitation of order $n_k \sim k$ to achieve a given probability amplitude. When it is off resonance, a larger gap tends to diminish the transition probability, which simply reflects the fact that atoms with larger energy gaps are harder to excite.

Some of these results are shown in Fig. 8. A notable result upon comparison of the two figures is that one can indeed amplify the transition probability by considering gaps that are "close" to the excited field state frequency. In Fig. 8, by considering the "off-resonant" gap at $\Omega = 3\pi/L \pm \epsilon$, there are regimes of acceleration in which the massive fields have better transition probabilities for both the accelerating detector and cavity scenarios than do their massless counterparts, and vice versa depending on whether $\Omega = \omega_n - \epsilon$ or $\Omega = \omega_n + \epsilon$ (in the plots, $\epsilon = 0.5\pi/L$). However, for each mass the distinction between an accelerating detector and an accelerating cavity quickly vanishes for small a.

Here we make a parenthetical comment that the relative magnitude of $\Omega - \omega_k$ or Ω/ω_k *does matter*: for a given

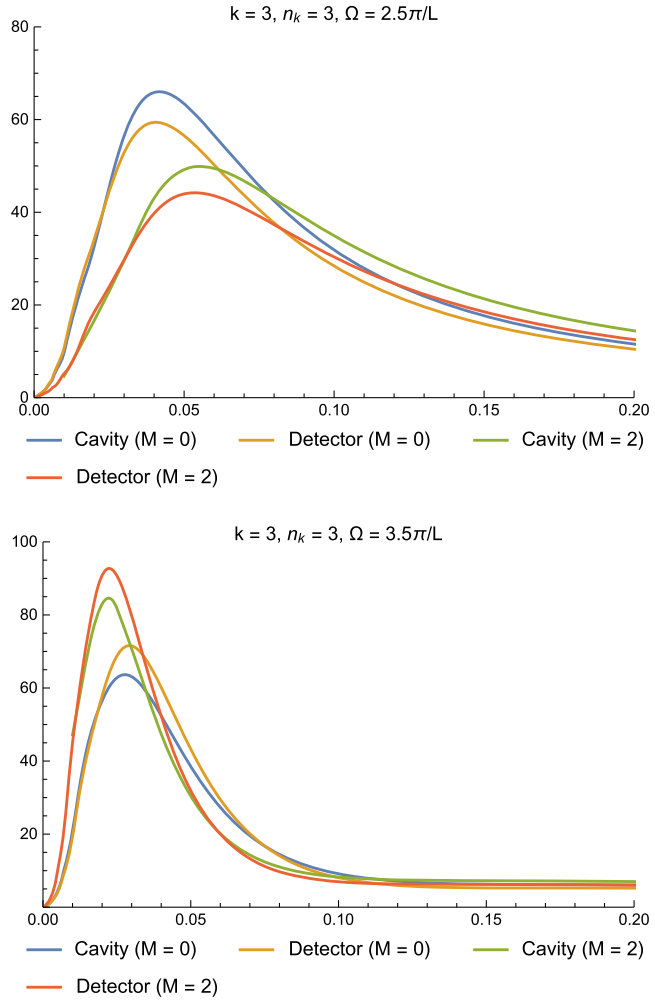

FIG. 8. Transition probability (divided by λ^2) as a function of acceleration for two different gaps, comparing the massless and massive cases. The field is in the third excited state i.e., $k = 3$ and we chose $n_3 = 3$. Top: $\Omega = 2.5\pi/L$. Bottom: $\Omega = 3.5\pi/L$. The plots are for $L = 1$.

fixed atomic gap Ω, one can engineer a situation in which massive fields can have a larger transition probability than the massless counterpart using resonance and vice versa. This is already apparent in Fig. 8 for small a, where the transition probability for the massive case can be lower or higher than the massless case depending on the choice of the gap Ω. This is, however, a separate problem from fundamentally distinguishing local accelerations.

The relative magnitude matters less as one moves away from resonance, e.g., when $\Omega/\omega_k \gg 1$. We check this for the case of a highly populated field state $n_k \gg 1$ as shown in Fig. 9, where we choose $k = 1$ and $n_k = 1000$ to match the setup in Ref. [3] for convenience. In the top panel, the massive field seems to outperform the massless case with regards to distinguishing local accelerations. However, this can be attributed to the resonant effect, since for our choice of fixed Ω, the magnitude of $\Omega - \omega_k$ is smaller for

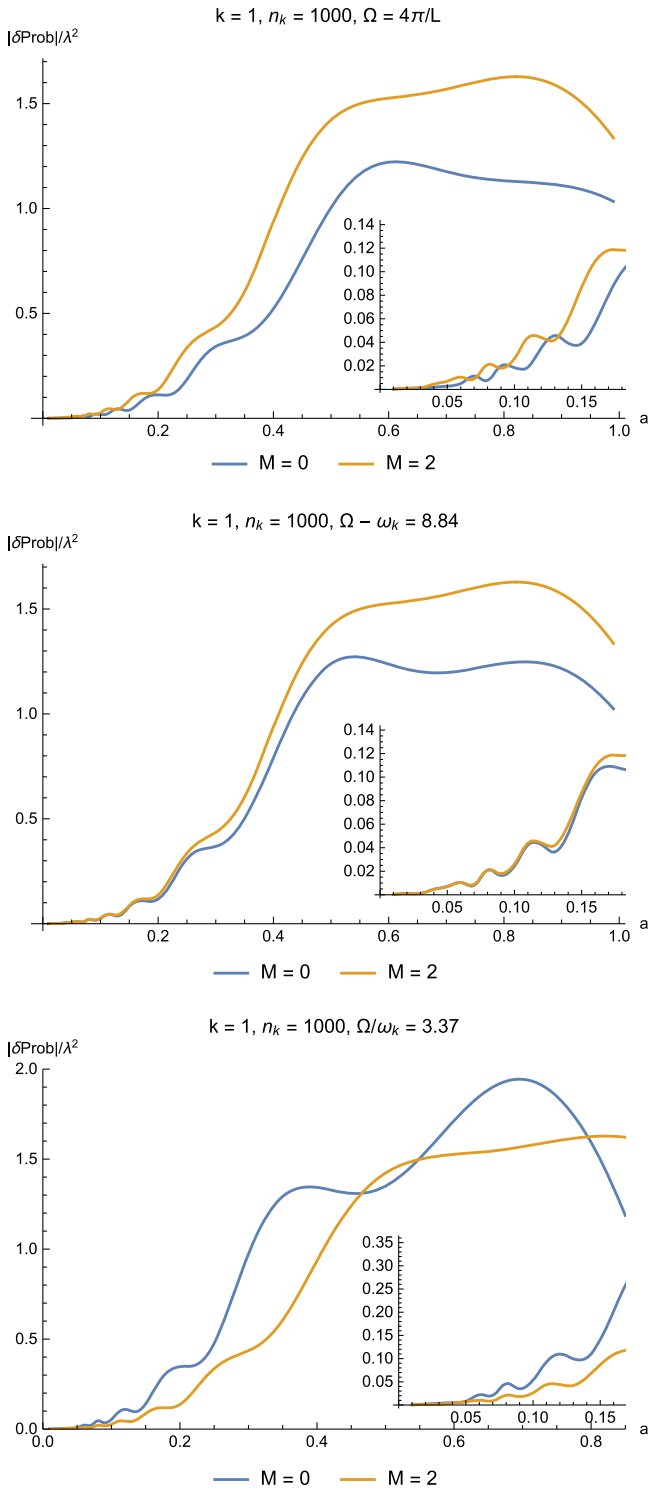

FIG. 9. Absolute probability difference (divided by λ^2) as a function of acceleration for large n_k. The field is in the third excited state i.e., $k = 3$ and we chose $n_3 = 3$. Top: $\Omega = 4\pi/L$. Middle: $\Omega - \omega_k = 8.84$ where the reference ω_k is chosen to be the angular frequency for the massive case. Bottom: $\Omega/\omega_k = 3.37$. The plots are for $L = 1$.

the massive case than for the massless case. A possibly fairer comparison would be to use the same $|\Omega - \omega_k|$ or Ω/ω_k, as shown in the middle and bottom panels of Fig. 9. When this is done, we see that the apparent advantage of the massive field over the massless one disappears and the massless field seems to perform equally well if not better.[4]

We conclude from these plots that massive fields do not seem to offer any obvious fundamental advantages at low accelerations as compared to their massless counterparts. In Appendix B we suggest a possible reason for the disparity with the results found in Ref. [3].

B. Coherent field state

An interesting case to consider is when the field is in a coherent state, analogous to that of a laser field in quantum optics scenarios. It is defined as the continuum limit of a quantum-mechanical coherent state for a quantum harmonic oscillator using the displacement operator $\hat{D}_{\alpha(k)}$ (see, for instance Ref. [13]):

$$|\alpha(k)\rangle := \hat{D}_{\alpha(k)}|0\rangle = \exp\left[\int \mathrm{d}k[\alpha(k)\hat{a}_k^\dagger - \alpha^*(k)\hat{a}_k]\right]|0\rangle. \quad (37)$$

Here $\alpha(k)$ is the *coherent amplitude distribution* defining a coherent amplitude for every mode k. As a coherent state, it satisfies the "eigenvalue" equation

$$\hat{a}_{k'}|\alpha(k)\rangle = \alpha(k')|\alpha(k)\rangle, \quad (38)$$

noting that $|\alpha(k)\rangle$ does not mean an explicit dependence on k but rather on the coherent amplitude distribution $\alpha(k)$. In a cavity, the spectrum becomes discrete and so we label the modes with integers n instead (e.g., the continuous variable k becomes discrete: $k_n = n\pi/L$ in the static cavity scenario). The coherent state has a simpler form

$$|\alpha(n)\rangle = \exp\left[\sum_{n=1}^{\infty}(\alpha_n\hat{a}_n^\dagger - \alpha_n^*\hat{a}_n)\right]|0\rangle. \quad (39)$$

Note that in this case we can formally write

$$|\alpha(n)\rangle \sim |\alpha_1\alpha_2\ldots\alpha_j\ldots\rangle \sim \bigotimes_{n=1}^{\infty}|\alpha_n\rangle \quad (40)$$

[4]This issue is somewhat tricky since it is uncertain which comparison is fairer. However, this "fairness" is necessary for the WEP since a fair comparison is analogous to "not being able to look out of the window of a rocket" to decide the asymmetry of the problem.

which denotes the tensor product of coherent states each with a complex coherent amplitude α_j. For a single-mode coherent state, say for the jth momentum, we have [cf. Eq. (38)]

$$\hat{a}_j|\alpha(k)\rangle = \alpha_j\delta_{jk}|\alpha(k)\rangle, \quad \alpha_j \in \mathbb{C}. \tag{41}$$

For a countably infinite multimode coherent state above, we require that

$$\sum_{n=1}^{\infty}|\alpha_n|^2 < \infty \tag{42}$$

which means that modes with higher momenta have a suppressed coherent amplitude. Here we will not employ the infinite multimode coherent state, and instead focus specifically on the more realistic single-mode coherent state as is used in quantum optics.

The Wightman function for the coherent state reads

$$\begin{aligned}W(\mathsf{x},\mathsf{x}') &= \langle 0|\hat{D}^{\dagger}_{\alpha(n)}\phi(\mathsf{x})\phi(\mathsf{x}')\hat{D}_{\alpha(n)}|0\rangle \\ &= \sum_{n=1}^{\infty}u_n(\mathsf{x})u_n^*(\mathsf{x}') + \sum_{n=1}^{\infty}\sum_{j=1}^{\infty}\alpha_n^*\alpha_j u_j(\mathsf{x})u_n^*(\mathsf{x}') \\ &\quad + \sum_{n=1}^{\infty}\sum_{j=1}^{\infty}\alpha_n\alpha_j^* u_j^*(\mathsf{x})u_n(\mathsf{x}') \\ &\quad + \sum_{n=1}^{\infty}\sum_{j=1}^{\infty}\alpha_n\alpha_j u_j(\mathsf{x})u_n(\mathsf{x}') \\ &\quad + \sum_{n=1}^{\infty}\sum_{j=1}^{\infty}\alpha_n^*\alpha_j^* u_j^*(\mathsf{x})u_n^*(\mathsf{x}').\end{aligned} \tag{43}$$

Note that similar to the single-mode excited Fock state, the vacuum contribution to the Wightman function does not vanish. If we define the one-point function of the coherent state as

$$J(\mathsf{x}) \coloneqq \langle\alpha(n)|\phi(\mathsf{x})|\alpha(n)\rangle = \sum_n \alpha_n u_n(\mathsf{x}), \tag{44}$$

we can compactly write the full Wightman function as

$$\begin{aligned}W(\mathsf{x},\mathsf{x}') &= W_0(\mathsf{x},\mathsf{x}') + J(\mathsf{x})J(\mathsf{x}') + J(\mathsf{x})J^*(\mathsf{x}') \\ &\quad + J^*(\mathsf{x})J(\mathsf{x}') + J^*(\mathsf{x})J^*(\mathsf{x}') \\ &= W_0(\mathsf{x},\mathsf{x}') + W_c(\mathsf{x},\mathsf{x}'), \\ W_c(\mathsf{x},\mathsf{x}') &= 4\mathrm{Re}[J(\mathsf{x})]\mathrm{Re}[J(\mathsf{x}')].\end{aligned} \tag{45}$$

The fact that $W_c(\mathsf{x},\mathsf{x}')$ factorizes into a product of one-point functions allows us to simplify the expression for the transition probability. The transition probability due to the purely coherent part [i.e., modulo the vacuum contribution $W_0(\mathsf{x},\mathsf{x}')$] then reads

$$\begin{aligned}\mathcal{P}_c(\Omega) &= \lambda^2\int \mathrm{d}\tau\mathrm{d}\tau'\chi(\tau)\chi(\tau')e^{-i\Omega(\tau-\tau')}W_c(\tau,\tau') \\ &= 4\lambda^2\left|\int \mathrm{d}\tau\chi(\tau)e^{-i\Omega\tau}\mathrm{Re}[J(\mathsf{x}(\tau))]\right|^2.\end{aligned} \tag{46}$$

With a judicious choice of $\{\alpha_n\}$, it may be possible to perform the infinite sum in $J(\tau)$ exactly. Before we proceed, it is worth noting that resonant behavior similar to that of the previous section is expected, since the real part of $J(\tau)$ contains a $\cos\omega_n t(\tau)$ term which produces a corotating term when combined with the exponential of the gap $e^{-i\Omega\tau}$.

For the single-mode coherent state, there is no real restriction on the coherent amplitude; we obtain

$$J(\mathsf{x}) = \delta_{mn}\sum_n \alpha_n u_n(\mathsf{x}), \tag{47}$$

where the mth mode is the coherent state and the rest are all vacuum modes. For simplicity we can consider, e.g., $m = 2$ and restrict $\alpha \in \mathbb{R}$ (though α can be an arbitrary complex number).

In Fig. 10 we illustrate the case when the second mode $k = 2$ is in a coherent state with coherent amplitude $\alpha_2 = 1$ while others are in the vacuum state. We also intentionally adjust the energy gap of the detector so that $\Omega = 1.9\omega_n$, which is different for massless and massive fields. This comparison can be thought of as being somewhat fairer since the amount by which the atom is off resonant from the mode frequency is of the same weight. We see that even with massive fields, the overall behavior remains unchanged and as expected, the transition amplitude degrades with larger mass. This contrast is even more apparent when we compute the absolute probability difference between the accelerating cavity and accelerating detector in massive and massless fields, as shown in Fig. 11. While we do not probe extremely nonrelativistic regimes due to computational resources, it is clear that the role of mass is vanishingly small for smaller acceleration. We have ignored the vacuum contribution because we have chosen the value of Ω such that the vacuum contribution is negligible compared to the contribution due to the excited field state. Furthermore, we have shown that vacuum states are not sensitive to local accelerations.

We pause to comment that the response of an accelerating cavity "underperforms" relative to an accelerating detector for a fixed mass m for large accelerations. We see in Fig. 8 that this under-/overperformance is reversed for $a \lesssim 0.35$. This can presumably be attributed to nonlinearities introduced by nonuniform acceleration across the accelerating cavity, though we do not yet have a full understanding of this effect.

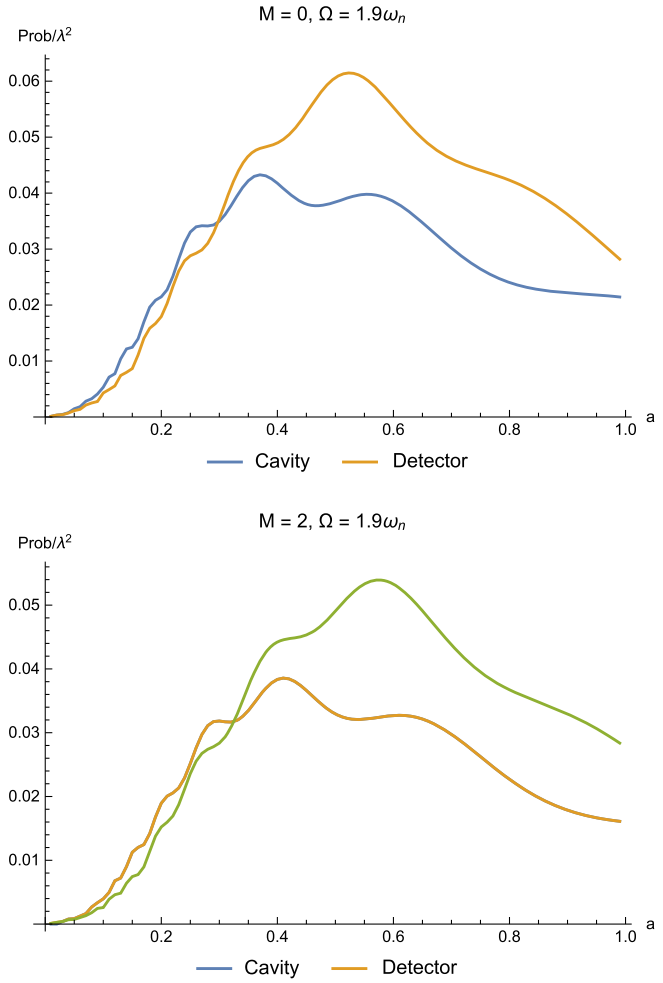

FIG. 10. Transition probability (modulo the vacuum contribution) for an accelerating detector and an accelerating cavity for two different masses when the second mode ($k = 2$) is in a coherent state and other modes are in vacuum states. In these plots $L = 1$.

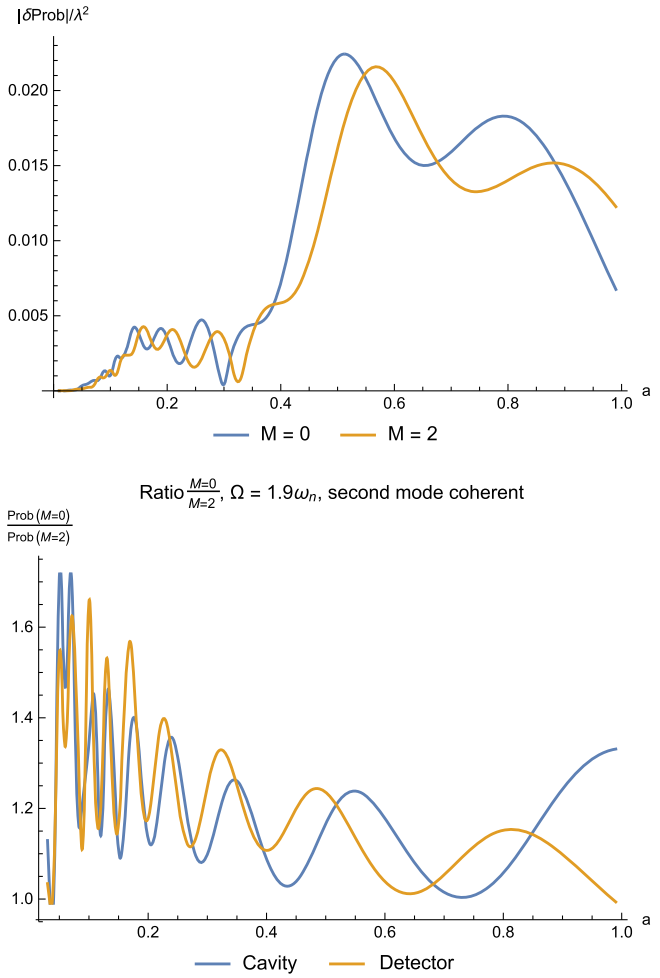

FIG. 11. Top: Absolute probability difference $|\delta P|/\lambda^2 = |P^C(\Omega) - P^D(\Omega)|/\lambda^2$ (modulo the vacuum contribution) for massless and massive fields. The difference is vanishing for small a regardless of mass. Bottom: The ratio of probabilities between massless and massive fields. We see that in low-acceleration regimes the ratio approaches 1.

C. Resonance

The resonance phenomenon, while not very exact due to the accelerated motion of the detector or cavity, can be made manifest if we study the "resonance peak" of the detector. The resonance peak for the case of the field in a Fock state $|n_k\rangle$ is shown in Fig. 12. Recall that in this notation, it is the kth momentum that has n_k excitations: if the field is in the seventh excited state with 20 excitations, then we write $|20_7\rangle$.

From Fig. 12 we observe that for large acceleration there is a larger Doppler shift, which smears out resonance and damps the transition probability. The number of resonance peaks matches the mode number k that defines the excited state of the field. As the acceleration decreases, the resonance peaks becomes narrower and higher, indicating that we approach resonance in the static inertial scenario. Figure 12 also shows that resonance dominates when

$$\Omega\tau \approx \lim_{a\to 0} \omega_k t(\tau), \tag{48}$$

where $t(\tau)$ is the pullback of the coordinate time in terms of the proper time τ of the detector. Crucially, the rough estimate of the right-hand side gives

$$\omega_k t(\tau) \approx \frac{k\pi}{aL}(a\tau + O(a^3\tau^3)) \sim \frac{k\pi\tau}{L} + O(a^3\tau^3), \tag{49}$$

which is to first order the same as the case for a static detector and static cavity.

We remark that near resonance $\Omega - \omega_k \approx 0$, Fig. 12 seems to indicate that the probability amplitude may be divergent if a is small enough, since λ^2 may not be small enough to make the probability amplitude less than 1 (e.g., set $\lambda = 0.1$). We expect this to be an artifact of the approximations in the whole setup, including perturbative

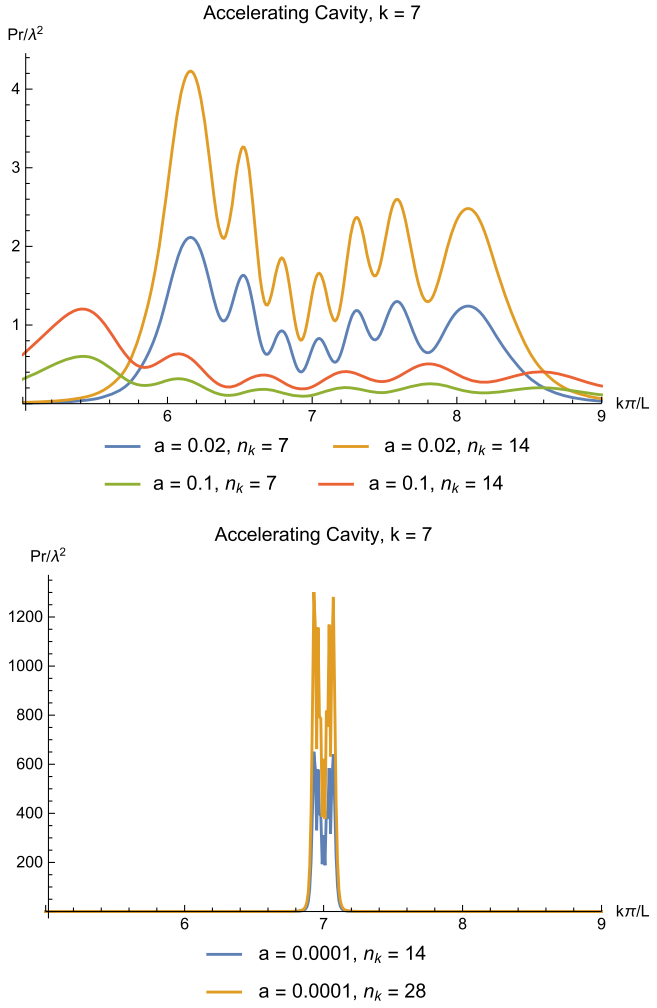

FIG. 12. Transition probability for fixed acceleration as a function of energy gap $\Omega = k\pi/L$ where n is real and n_k is the number of excitations of the massless scalar field in mode k, with $L = 1$.

calculations of the transition probability $P(\Omega)$. As an example of such artifacts, note that in Eq. (34) the transition probability scales linearly with n_k (this also appeared in Ref. [3]). Clearly, this cannot be valid for arbitrary n_k since for large enough excitations, the probability can be made greater than 1. These may be canceled by higher-order terms which would also contain corotating terms. Also, recall that since our detector starts from one end of the cavity, in the limit where $a = 0$ we should expect *no excitation* at all due to Dirichlet boundary conditions given the choice of coupling. This suggests that for computations involving nonvacuum contributions and corotating terms, one should be careful in extrapolating results.

Nonetheless, our results so far do not change even if we stay away from the $\Omega \approx \omega_k$ limit (cf. Fig. 10), since all that the resonance condition and large-n_k limit do is allow us to ignore vacuum contributions from $W_0(\tau, \tau')$ by amplifying the nonvacuum contributions. Even if the excited parts W_{exc}, W_c of the Wightman function are smaller than W_0, we could simply subtract off the W_0 part since we find a negligible difference between the responses in Experiment 1 and Experiment 2.

VII. TRANSITION RATE

The computation of a transition probability—also known as a *response function* $F(\Omega)$ of a particle detector with energy gap Ω—as a detector traverses through a quantum field coupled to it has a physical interpretation: it provides an operational way of defining the particle content of the field without invoking a high degree of spacetime symmetry [20,21]. However, the fact that it is a double integral may obscure information about the atom-field interaction. This prompts us to consider whether the *transition rate*, essentially the time derivative of the response function along the detector trajectory, can provide further insights into the WEP.

To obtain the response rate, we need to rewrite the response function in such a way that it can be easily differentiated. This is done by changing variables [22]

$$F(\Omega) = 2\text{Re}\int_{\tau_0}^{\tau} du \int_0^{u-\tau_0} ds e^{-i\Omega s} W(u, u-s), \tag{50}$$

where τ_0 denotes the time at which the detector is switched on. Instead of the usual response function which gives the transition probability of exciting the atom from its ground state, we can now compute the *instantaneous transition rate* of a detector turned on at time τ_0 and read at time τ, given by [22]

$$\dot{F}(\Omega) = \frac{dF(\Omega)}{d\tau} = 2\text{Re}\int_0^{\tau-\tau_0} ds e^{-i\Omega s} W(\tau, \tau-s). \tag{51}$$

Despite some subtleties in handling this observable for free space involving regularization, we expect that the cavity setup removes these difficulties since the field is compactly supported and there is an infrared cutoff. In our scenario it is convenient to compute the case where $\tau_0 = 0$. If different field states have a chance of causing different responses in the detector, the transition rate may be able to pick this up.[5] Conversely, if the transition rates are identical, then the response of the detector should be the same under integration.

Since the response rate is linear in $W(\tau, \tau')$, we will split it into two parts:

$$\dot{F}(\Omega) = \dot{F}_0(\Omega) + \dot{F}_1(\Omega) \tag{52}$$

where $\dot{F}_0$ is the vacuum contribution and $\dot{F}_1$ is the remaining contribution due to the field in an excited state.

[5]On the other hand, it is possible that the response function washes out differential differences due to the mean value theorem.

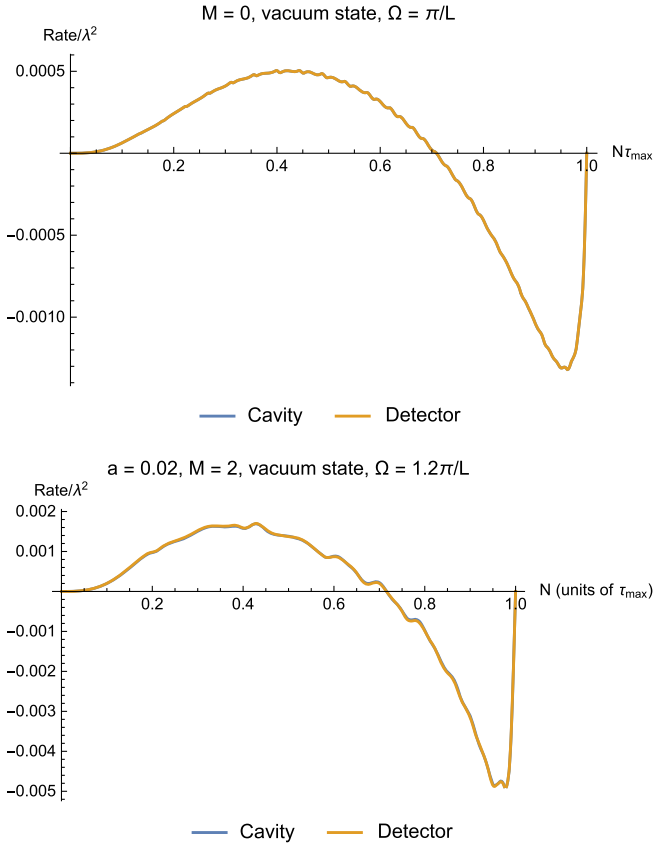

FIG. 13. Transition rate as a function of time τ. Note that in both cases the transition rates for the accelerating cavity and accelerating detector scenarios are practically indistinguishable regardless of mass. We chose different parameters for variations.

The vacuum state transition rate is shown in Fig. 13. The crucial thing to note here is that the vacuum contributions for both cases have negligible differences in their transition rates; therefore the transition probability must be the same as well after integrating across the full trajectory. To save computational time, we chose $a = 0.02$ to represent the massive case and the same conclusion holds. This justifies our earlier results (as well as those in Ref. [3]) that vacuum contributions are not sensitive to local accelerations.

Two examples of a highly populated first excited state ($k = 1$, $n_k = 100$) for the massless case are shown in Fig. 14. We see that while the rate appears qualitatively different at different read-out times, the *difference* between an accelerating cavity and an accelerating detector is very small (of course it is only exactly zero for a static setup). As far as differences go, massive fields generically do not perform better than massless ones, which is consistent with the idea that the role of mass tends to "kill off" correlations at large distances and diminish the amplitudes.

From Fig. 14, one might be led to think that a massive field seems to have a *very large* response rate compared to a massless field, but this is not the right comparison. Note that the corotating frequency $\Omega - \omega_n$ determines quite

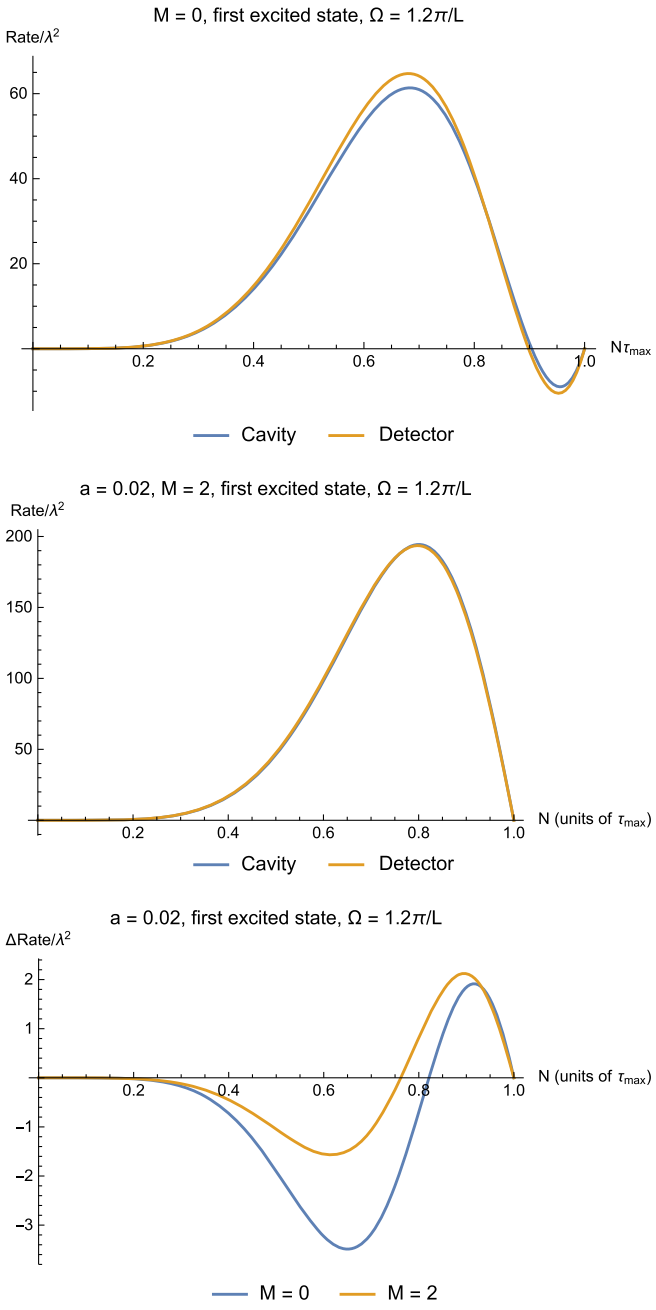

FIG. 14. Transition rate as a function of time τ for the first excited state of the field. Top: Massless case. Middle: Massive case. Bottom: Difference in transition rate for both scenarios. It appears that the transition rate and hence transition amplitude are slightly more advantageous for the massless case for a given acceleration. Here "ΔRate" is simply $\Delta\dot{F} = \dot{F}^D = \dot{F}^C$.

directly the magnitude of these rates, and given the same gap Ω, one of the two fields will be closer to the "resonant frequency" than the other. In Fig. 15, we adjust the gap so that for both massless and massive fields the atomic gap is $\Omega = 1.012\omega_1$, where ω_1 is the frequency of the first mode. As expected, the absolute value of the transition rate for massless fields dominates the massive case. The difference

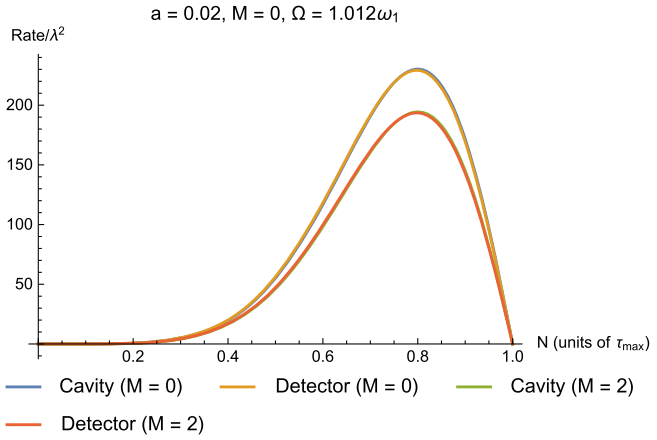

FIG. 15. Transition rate as a function of time τ for the first excited state of the field. Top: Massless case. Middle: Massive case. Bottom: Difference in transition rate for both scenarios. It appears that the transition rate and hence transition amplitude are slightly more advantageous for the massless case for a given acceleration.

in response rates $\Delta\dot{F} = \dot{F}^D - \dot{F}^C$, where C, D denote the accelerating cavity and detector respectively, are of approximately the same order as seen in Fig. 15.

With hindsight we should not be surprised by these results, since they are basically an Unruh-type setup confined to a cavity. As clarified in Ref. [2], what is important in these WEP considerations is really the fact that there is *relative acceleration* between the atom and the cavity. In the slow-acceleration limit, every point in the cavity can be approximated to have the same constant proper acceleration (hence the same clock ticking rates) and so an accelerating cavity–static detector and an accelerating detector–static cavity should lead to the same physical results. The mass parameter of the scalar field enters the quantum field via the mode frequency and amplitude, which generally degrade response since the integral over the Wightman function is more oscillatory and the normalization for each mode is smaller than those for a massless field. In this respect, if a "fair" comparison is made between the massless and massive cases (e.g., adjusting Ω/ω_k or $|\Omega - \omega_k|$ instead of fixing Ωl, cf. Sec. VI), the massless field should lead to larger detector responses because mass suppresses nonlocal correlations. Note that this suppression is *independent* of the WEP.

Why would the responses be different at large a? As argued in the context of mirrors [2], the accelerating cavity–static detector and the accelerating detector–static cavity setups are also not mathematically equivalent: if our experiments are sensitive enough to nonuniformity of acceleration across the cavity, then the notion of "relative acceleration" becomes blurred. For an accelerating detector, in the cavity frame one observes that the detector has a constant-acceleration trajectory; for an accelerating cavity, in the cavity frame one observes that the detector is not uniformly accelerating because its worldline crosses all the hypersurfaces of constant ξ between one cavity wall $\xi = \xi_2$ and another $\xi = \xi_1$. In the slow-acceleration limit, these constant-ξ surfaces describe approximately the same acceleration and hence the detector is observed to be approximately uniformly accelerating. We can think of the correlation functions of the field as capturing this nonlocal difference and the inequivalent setups lead to unequal responses. It is in this spirit that the WEP makes sense: the responses between the free-falling cavity–stationary detector and free-falling detector–stationary cavity will be different once the nonuniformity of the gravitational field is detectable.

Finally, a small qualification about the comparison between the two different scenarios (accelerating detector and accelerating cavity) is in order. There are a couple of ways in which the two scenarios can be argued not to be on equal footing. First, we note that in relativity there is no absolute rigidity [9–11]; it is impossible to maintain fixed coordinate distance between two cavity walls in *all frames*. Accelerating the cavity while keeping it rigid in the cavity rest frame (Fermi-Walker rigidity) is the simplest and most natural setup. The fact that for accelerating cavities the detector is seen to be nonuniformly accelerating from the cavity's frame, is sufficient to show that the detector response should be different from the constantly accelerating detector scenario.

However, there is also a perhaps more fundamental and easier argument for the lack of equivalence between the two scenarios: the accelerating cavity is a setup of accelerating mirrors, which are perfectly reflecting boundary conditions, whereas an accelerating detector is a quantum object that can absorb, transmit and reflect parts of an illuminating plane wave. Consequently, they constitute rather distinct field configurations (e.g., dynamical Casimir effect and Unruh radiation respectively) and the two setups are not identical beyond the "nonuniformity" of the acceleration either. We can estimate the deviation between the two scenarios e.g., from Eq. (49), which can be seen to be third order in the dimensionless parameter that depends on acceleration and the duration of the interaction.

VIII. CONCLUSION

We have investigated a quantum version of the WEP in which we considered the response of a particle detector in two scenarios: a) a detector accelerating in a static cavity and b) a static detector in an accelerating cavity. We found that the qualitative WEP is indeed satisfied insofar as quasilocal approximations are valid. We did this by investigating the transition probability of a two-level atomic detector on various field states, namely a vacuum state (Minkowski-like and Rindler-like vacuum), an arbitrary Fock state, and a single-mode coherent state. We also checked the effect of bringing the atomic gap closer to the resonant frequency when we have corotating terms and clarified the validity of some approximations such as the

large-n_k limit for the Fock state of the field. Importantly, the results support the idea that a "quantum accelerometer" in the nonrelativistic regime would work equally well for massless and massive fields. We strengthened the results by computing the transition rates to ensure that no fundamental physical differences were averaged out by integration when we computed transition probabilities. In this sense, our results complement those of Refs. [2,6].

ACKNOWLEDGMENTS

This work was supported in part by the Natural Sciences and Engineering Research Council of Canada. E. T. thanks Jorma Louko, Robie Hennigar and Richard Lopp for useful discussions and A. Dragan for helpful correspondence. E. M.-M. also acknowledges funding form his Ontario Early Researcher Award.

APPENDIX A: SOLVING THE MASSLESS KLEIN-GORDON EQUATION WITHOUT CONFORMAL TRANSFORMATION

In this section we solve for the solution for the massless Klein-Gordon (KG) field equation without invoking conformal transformation of any sort. We quote again the standard Rindler coordinates for convenience:

$$t = \xi \sinh\eta, \qquad x = \xi \cosh\eta.$$

The general Klein-Gordon field equation [cf. Eq. (1)] in this coordinate system gives the modified Bessel differential equation for the spatial modes $v(\eta, \xi)$:

$$\xi^2 \frac{\mathrm{d}^2 v}{\mathrm{d}\xi^2} + \xi \frac{\mathrm{d}v}{\mathrm{d}\xi} + (\omega^2 - m^2\xi^2)v = 0. \tag{A1}$$

The solution basis for $m \neq 0$ is given by $\mathrm{Re}(I_{i\omega})$ and $K_{i\omega}$ which are both real and linearly independent due to the nontrivial Wronskian [19]. Now let us set $m = 0$ in Eq. (A1). The eigenbasis[6] of the solution space is given by $\sin(\omega \log\xi)$ and $\cos(\omega \log\xi)$. Note that we could also obtain this by doing a series expansion for small $m \to 0^+$ on the mode solutions in Eq. (27) which satisfies the Dirichlet boundary condition at $\xi = \xi_1$ [19]. Since η is dimensionless, here ω is as well. If we let the boundary conditions be at $\xi_1 = a^{-1}$ and $\xi_2 = a^{-1} + L$, we get

$$v_n \propto \sin(\omega_n \log\xi) - \tan\left(\omega_n \log\frac{1}{a}\right)\cos(\omega_n \log\xi), \tag{A2}$$

where ω_n is now a discrete spectrum due to the second boundary condition $\xi = \xi_2$. The normalization can be found using the standard Klein-Gordon inner product [8]. Remarkably, even after imposing the second boundary condition, the spectrum is still exact, which reads

$$\omega_n = \frac{n\pi}{\log(1 + aL)}, \qquad n \in \mathbb{N}, \tag{A3}$$

which is precisely what we got from the conformal transformation where we identify the denominator as aL', the conformally transformed length of the cavity multiplied by the kinematical parameter a. In some sense this is perhaps not surprising, since the same physical situation should be described by the same differential operator with the same set of spectra (which is invariant under coordinate transformations).

Some representative plots of the modes for small and large accelerations are given in Fig. 16. Now it is very clear that the spatial modes approach the Minkowski static cavity scenario very quickly for not too small $a \sim 0.01$, while for large acceleration (of the left wall) the modes are "deformed sine functions." These deformed modes are in fact very similar in form to the modes for the massive case described in terms of modified Bessel functions of imaginary order $\mathrm{Re}(I_{i\omega})$ and $K_{i\omega}$.

This clearly demonstrates that the differential equation governing the form of the spatial modes is solvable directly even if the metric is not the one conformally equivalent to the Minkowski metric. In the standard Rindler coordinates, the Klein-Gordon equation would also not be conformally invariant under the change of coordinates. However, the standard Rindler coordinates and conformal Rindler coordinates both cover the Rindler wedge portion of Minkowski spacetime and each hypersurface of constant ξ in either system of coordinates describes the trajectory of uniformly accelerating test particles. One would not conclude that massless fields cannot distinguish the two scenarios on grounds of conformal invariance, while massive fields can; instead, one would conclude that both should have qualitatively similar behavior up to some degradation factor due to the mass of the field that enters the normalization constant and phase factor in the integral of the transition probability.

Here we make a short remark on the distinction between conformal flatness and conformal invariance of field equations via a conformal transformation. A spacetime M is said to be conformally flat if *there exists* a coordinate system in which the metric can be rewritten as

$$g_{\mu\nu}(\mathsf{x}) = \Omega(\mathsf{x})^2 \eta_{\mu\nu}, \tag{A4}$$

and in $(1 + 1)$ dimensions all Lorentzian manifolds are conformally flat. The massless KG field is conformally invariant because under conformal transformation, the KG equation takes the same form as the wave equation in global

[6]This is not the one used in e.g., Refs. [3,23], but for our purposes either one will work. Roughly speaking, one can check from the series expansion at small m that this is analogous to the choice of writing solutions of the harmonic oscillator equation in terms of cosine/sine functions or plane waves.

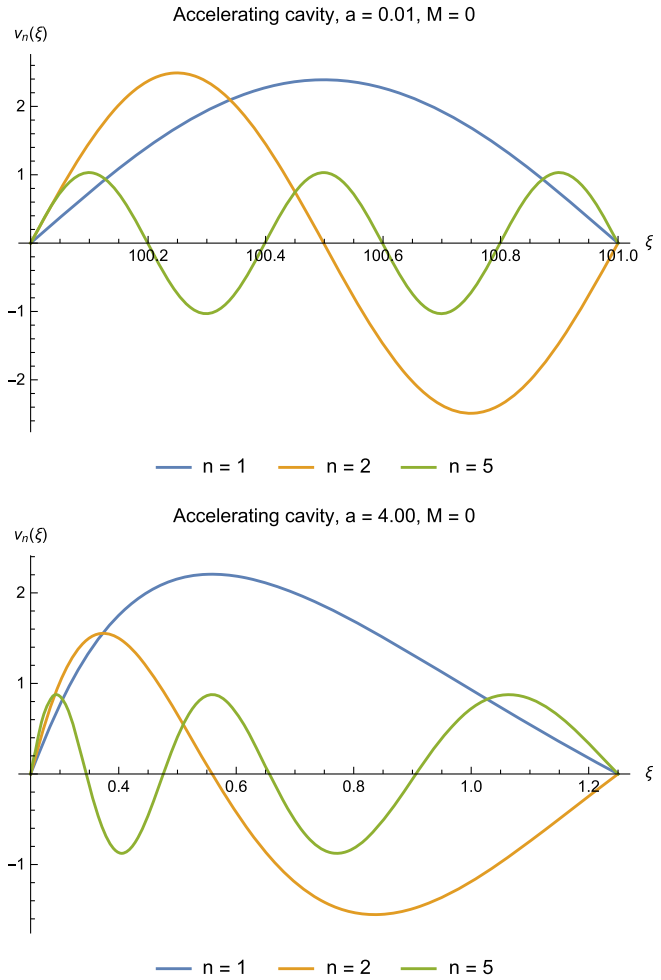

FIG. 16. Sample plots of mode functions for the second mode $n = 2$ for small and large accelerations. This makes clear that the large-acceleration limit is "Bessel-like," in that the mode function is a deformed sine function, squashed in the direction of acceleration. These plots are not normalized since we are concerned with their forms rather than their amplitudes.

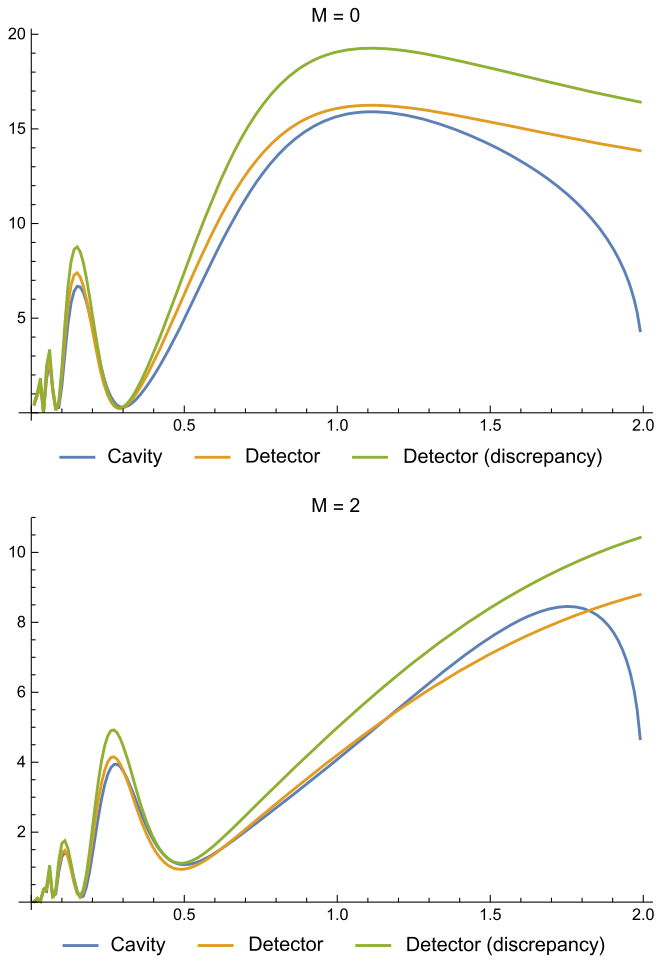

FIG. 17. The transition probability plot simulating the plots found in Ref. [3]. The discrepancy is possibly related to incorrect normalization for the massive field–accelerating detector scenario (labeled "discrepancy" here), thus producing the result that massive fields can better distinguish local acceleration.

Minkowski coordinates. However, performing a conformal transformation is a calculational advantage that does not change the physics, since we could equally do physics using a nonconformally equivalent metric that describes the same spacetime. Alternatively, we say that the physics is contained in $\Omega(\mathsf{x})$ and so the physics will still be different from static Minkowski spacetime [2]. A good example is the de Sitter expanding universe, which can be written in coordinates such that it is conformally flat: the mode functions inherit the form in flat space, but a static detector in the conformal vacuum of the de Sitter spacetime detects particles while the static detector in the Minkowski vacuum does not.

APPENDIX B: DISCREPANCY WITH PAST RESULTS

Based on the argument above, there is a slight disparity between the results obtained here and the results obtained in Ref. [3]. Since the exact parameters used previously [3] are unknown, we attempt to emulate the construction and the result is shown in Fig. 17. From what we can discern, this discrepancy arises from making the same (inappropriate) normalization choice for both the massive and massless cases. For a detector accelerating in a static cavity with a massive scalar field [3], this leads to the conclusion that (in the nonrelativistic regime) massive fields can distinguish local acceleration whereas massless fields cannot.

Despite the discrepancy, the results here and in Ref. [3] nonetheless show that detector responses can indeed detect nonuniformity of accelerations in a cavity which leads to distinguishability between the two scenarios. Essentially, it boils down to the fact that in the accelerating cavity scenario, the static detector is only approximately uniformly accelerating from the perspective of the cavity frame, since the vertical worldlines cross hypersurfaces of constant but different ξ, which is approximately constant for a very short cavity or very small accelerations. On the

other hand, an accelerating detector is an *exactly* uniformly accelerating test body; thus the setup is not mathematically equivalent—hence "qualitative weak equivalence principle" [2].

To summarize, we first note that both the accelerating cavity and accelerating detector setups are *kinematically inequivalent* for any nonzero aL, as illustrated in Sec. V and Appendix A. What conformal invariance in $(1+1)$ dimensions gives us is convenience, a point also made in Ref. [2]. It boils down to the fact that in the rest frame of an accelerating cavity the detector does *not* undergo uniform acceleration. Therefore, for any value of aL, there exists a finite difference in transition probability $\Delta\,\mathrm{Pr} = |\mathrm{Pr}_{\mathrm{cav}} - \mathrm{Pr}_{\mathrm{det}}|$ between the two setups regardless of the mass of the field. This difference quickly vanishes as $aL \to 0$: in this "quasilocal regime," we can approximate the whole cavity as accelerating with a single proper acceleration, recalling that the acceleration along the length of the cavity $a(x)$ is related to the acceleration of the rear wall a_1 by

$$a(x) = \frac{a_1}{1 + a_1(x - x_1)} \approx a_1 \tag{B1}$$

if $a_1(x - x_1) < a_1 L \ll 1$. For this reason, $\Delta\,\mathrm{Pr}$ falls quickly as $a \to 0$, becoming exactly zero when $a = 0$ (entirely static detector and cavity setups). So long as $aL \neq 0$, in principle we can always distinguish local accelerations using nonlocal correlations of the field regardless of mass. Choosing the detector gap to be closer to the resonant frequency of the field (e.g., excited Fock state) will help in amplifying very small transition probabilities, noting that the resonant frequencies between massless and massive cases would be different.

An alternative interpretation would be to require that if $\Delta\,\mathrm{Pr}$ is below a certain threshold we lose the capacity to distinguish local accelerations in the nonrelativistic regime. All things being equal (taking into account resonant effects, etc.), this would mean that generically neither massless nor massive fields can do the job of frame distinction if the threshold is not exceeded. While operationally sensible, we prefer the previous interpretation since $\Delta\,\mathrm{Pr}$ generally never actually vanishes except when both the cavity and the detector are at rest relative to one another. Neither massless nor massive fields are "preferred" in their capacity to distinguish local relative accelerations; any quantitative difference is purely due to quantum-theoretic aspects of nonlocal field correlations and their dependence on mass.

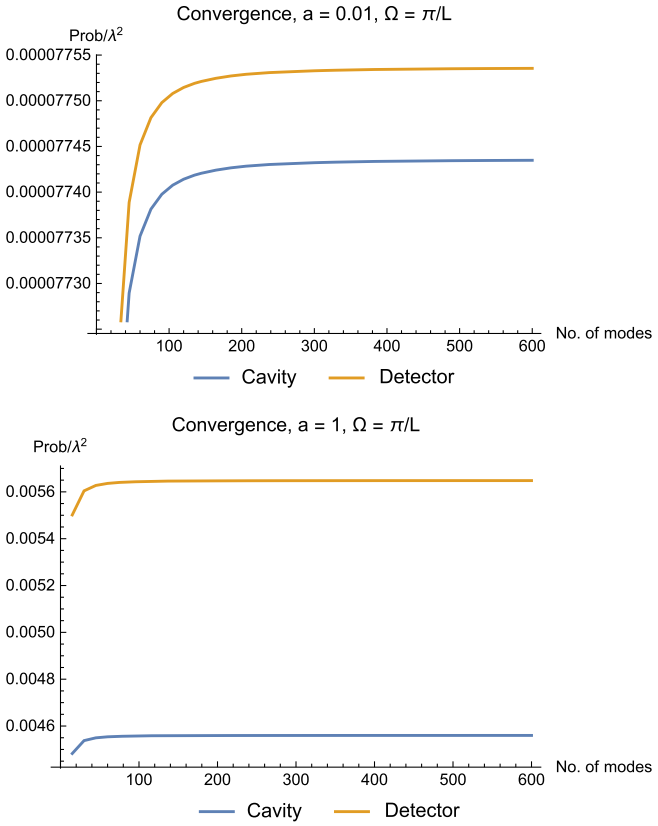

FIG. 18. Probability as a function of mode sum N for $a = 0.01$ and $a = 1.0$ with $M = 0$.

APPENDIX C: CONVERGENCE OF MODE SUMS

We show some plots demonstrating how quickly the mode sums converge for certain choices of parameters. In Fig. 18 we plot the transition probabilities as a function of mode sum for the field initiated as a vacuum state for two different accelerations a.

We see that the convergence is attained for relatively small $N \sim 100$, and even if we sum $N = 15$ (the smallest N in these plots), the values do not stray far from the converged value; thus for practical purposes we choose to perform calculations involving a vacuum state for $N = 15$. Note that for fields initiated in excited states, the Wightman function has vacuum and excited state contributions but the latter does not occur as sums over modes and hence the convergence issue do not appear.

[1] A. Pozas-Kerstjens and E. Martín-Martínez, Phys. Rev. D **94**, 064074 (2016).
[2] S. A. Fulling and J. H. Wilson, arXiv:1805.01013.
[3] A. Dragan, I. Fuentes, and J. Louko, Phys. Rev. D **83**, 085020 (2011).
[4] A. Ahmadzadegan, E. Martin-Martinez, and R. B. Mann, Phys. Rev. D **89**, 024013 (2014).
[5] A. Ahmadzadegan, R. B. Mann, and E. Martin-Martinez, Phys. Rev. A **90**, 062107 (2014).
[6] M. O. Scully, S. Fulling, D. Lee, D. Page, W. Schleich, and A. Svidzinsky, Proc. Natl. Acad. Sci. U.S.A. **115**, 8131 (2018).
[7] B. Schutz, *A First Course in General Relativity* (Cambridge University Press, Cambridge, England, 2009).
[8] N. Birrell, N. Birrell, and P. Davies, *Quantum Fields in Curved Space* (Cambridge University Press, Cambridge, England, 1984).
[9] G. Herglotz, Ann. Phys. (Leipzig) **31**, 393 (1910).
[10] F. Noether, Ann. Phys. (Leipzig) **31**, 919 (1910).
[11] R. J. Epp, R. B. Mann, and P. L. McGrath, Classical Quantum Gravity **26**, 035015 (2009).
[12] F. Kiałka, A. R. H. Smith, M. Ahmadi, and A. Dragan, Phys. Rev. D **97**, 065010 (2018).
[13] P. Simidzija and E. Martin-Martinez, Phys. Rev. D **96**, 025020 (2017).
[14] D. E. Bruschi, I. Fuentes, and J. Louko, Phys. Rev. D **85**, 061701 (2012).
[15] R. Lopp, E. Martín-Martínez, and D. N. Page, arXiv: 1806.10158.
[16] L. Sriramkumar and T. Padmanabhan, Classical Quantum Gravity **13**, 2061 (1996).
[17] L. Hodgkinson and J. Louko, J. Math. Phys. (N.Y.) **53**, 082301 (2012).
[18] H. Lass, Am. J. Phys. **31**, 274 (1963).
[19] DLMF, NIST Digital Library of Mathematical Functions, http://dlmf.nist.gov/, Release 1.0.18, edited by W. J. Olver, A. B. Olde Daalhuis, D. W. Lozier, B. I. Schneider, R. F. Boisvert, C. W. Clark, B. R. Miller, and B. V. Saunders.
[20] W. G. Unruh, Phys. Rev. D **14**, 870 (1976).
[21] B. S. Dewitt, in *General Relativity: An Einstein Centenary Survey,* edited by S. W. Hawking and W. Israel (Cambridge, University press, Cambridge, England, 1979), p. 680.
[22] J. Louko and A. Satz, Classical Quantum Gravity **25**, 055012 (2008).
[23] N. Friis, A. R. Lee, and J. Louko, Phys. Rev. D **88**, 064028 (2013).